11th ANKARA INTERNATIONAL AEROSPACE CONFERENCE **AIAC-2021-000**
8-10 September 2021 - METU, Ankara TURKEY

LAYOUT OPTIMIZATION OF DELTA CANARD-WING CONFIGURATION

Alp TIKENOGULLARI* and Kaan YUTUK†
METU
Ankara, Turkey

Ismail H. TUNCER‡
METU
Ankara, Turkey

ABSTRACT

Delta canard-wing configuration forms a fairly complex vortex structure and performs vortex interactions under the condition that placed close coupled in high angle of attack. As a result, wing and canard vortices creates a favorable effect on aerodynamics efficiency. This favorable effect make the optimization of canard position with respect to wing is a promising challenge for the modern aircraft. In this study, we present the results of our optimization study for canard position with respect to wing. With this study, optimum position of the canard is indicated under certain circumstances by using indigenous optimization framework, and it's effects on flow field around configuration with CFD solver, SU^2.

INTRODUCTION

Modern fighter aircraft have requirements on reaching high speeds, agility and sustained lift at high angles of attack as a consequence of high maneuverability demands. These requirements led a large number of investigations on delta wing due to its advantages on high lift enhancement at larger angles of attack, reducing compressibility effects and wave drag [Lee, 1989; Earnshaw, 1964; Gursul , 1995] and close-coupled canard-wing configurations in order to delay the wing stall at high angles of attack [Behrbohm, 1965; Bergmann, 1991; Oelker, 1989; Yutuk , 2021]. The experiments and numerical studies show that using a canard surface positioned appropriately in front of the wing has several advantages such as increase in $C_{L_{max}}$ and stall angle, higher trimmed lift capability and reduced trim drag. Canard surface may also be used to reduce or even negative the static stability and it can improve agility and maneuverability [Tu, 1992; Gloss, 1974]. Today, there are lots of aircraft having large variety of canard-wing configuration layout, in which canard is fixed or movable, located at various positions relative to wing, or placed at various incidence angles. These numerous layout options may be favorable or unfavorable, depending on the geometry and flight conditions. Therefore, it is essential to investigate different layout options at given flight conditions to utilize the canard-wing configuration at its optimum performance. There are several experimental and numerical studies [Gloss, 1975; Tu , 1994, 1996] on the effect of canard position and deflection angle but none of them conduct any optimization study. This study presented in this paper aims

*MSc. Student, Aerospace Engineering Department, Email: alp.tikenogullari@metu.edu.tr
†MSc. Student, Aerospace Engineering Department and Research Engineer, Turkish Aerospace, Email: yutuk.kaan@metu.edu.tr
‡Professor, Aerospace Engineering Department, Email: author3@work.com

constructing an optimization framework that can result the optimum close-coupled canard-wing configuration layout by deforming canard position at a given flight condition.

METHOD

Computational Grid

The whole computational domain is resolved by tetrahedral cells since inviscid flow assumption is employed in a unstructered FVM solver. An open source mesh generation tool kit, GMSH, is used to generate grids. GMSH has a grid generation feature based on scripts which are similar C++, and it allows automated mesh generation. By employing this feature, canard is automatically transformed (or deformed) due to the gradient calculated by SU2 and then re-meshing process is applied at each optimization step.

Grid convergence study is conducted by the solution-based grid adaptation methodology, available in SU^2. This methodology is suggested by Biswas and Strawn [Biswas , 1994, 1998] which uses anisotropic grid refinement technique and applied only to tetrahedral cells.

Flow Field Solver

In the current study, SU^2, version 6.2.0, is operated for the inviscid solutions of flow fields over a close-coupled canard-wing configuration. SU^2 is an open-source node-based finite volume solver which uses unstructured grids. Inviscid and turbulent flows are both described in the solver [Palacios, 2014]. The code is initially developed at Stanford University, and still being developed by a world-wide community. Moreover, SU^2 is also capable of solving adjoint sensitivities with the module `SU2_CFD_AD`.

The general form of governing PDE of Navier-Stokes equation can be defined in computational domain, $\Omega \subset \mathbb{R}^3$ as,

$$\partial_t U + \nabla \cdot \vec{F}_c(U) - \nabla \cdot \vec{F}_v(U) = Q \; in \; \Omega, t > 0 \tag{1}$$

where U stands for the flow variables vector in conservative form, $\vec{F}_c(U)$ and $\vec{F}_v(U)$ are the convective and viscous flux terms, relatively, and Q is a generic source term. Although equation (1) represents the general form, the flow solutions in this study are evaluated by employing steady-state, compressible and inviscid flow equations. Convecitve fluxes are evaluated by JST scheme. The gradients of variables are evaluated by Weighted Least Squares method. FGMRES iterative solver is employed in this study with ILU preconditioner for the solution of linear system.

A gradient-based optimization technique is employed in this study. Gradients are calculated by the discrete adjoint method which has been already implemented in the SU^2 solver. In this methodology, the sensitivity of objective function with respect to design variables are,

$$\frac{dJ}{dx} = \frac{\partial J}{\partial U}\frac{dU}{dx} + \frac{\partial J}{\partial x} \tag{2}$$

and similarly sensitivity of governing equation is

$$\frac{dR}{dx} = \frac{\partial R}{\partial U}\frac{dU}{dx} + \frac{\partial R}{\partial x} = 0 \tag{3}$$

or,

$$\frac{dU}{dx} = -\left(\frac{\partial R}{\partial U}\right)^{-1}\frac{\partial R}{\partial x} \tag{4}$$

substitute equation 4 into objective function,

$$\frac{dJ}{dx} = -\frac{\partial J}{\partial U}\left(\frac{\partial R}{\partial U}\right)^{-1}\frac{\partial R}{\partial x} + \frac{\partial J}{\partial x} \tag{5}$$

Define a Lagrange multiplier, ψ, which satisfies the following adjoint equation,

$$\left(\frac{\partial R}{\partial U}\right)^T \psi = -\left(\frac{\partial J}{\partial U}\right)^T \tag{6}$$

Then, sensitivity equation of objective function becomes

$$\frac{dJ}{dx} = \psi^T \frac{\partial R}{\partial x} + \frac{\partial J}{\partial x} \tag{7}$$

Therefore, objective function becomes independent of flow variables, and solving only two equations, one adjoint equation and one objective function is enough for gradient calculations, regardless of the number of design variables. On the other hand, the one has to solve adjoint equation for each objective function

Optimization Framework

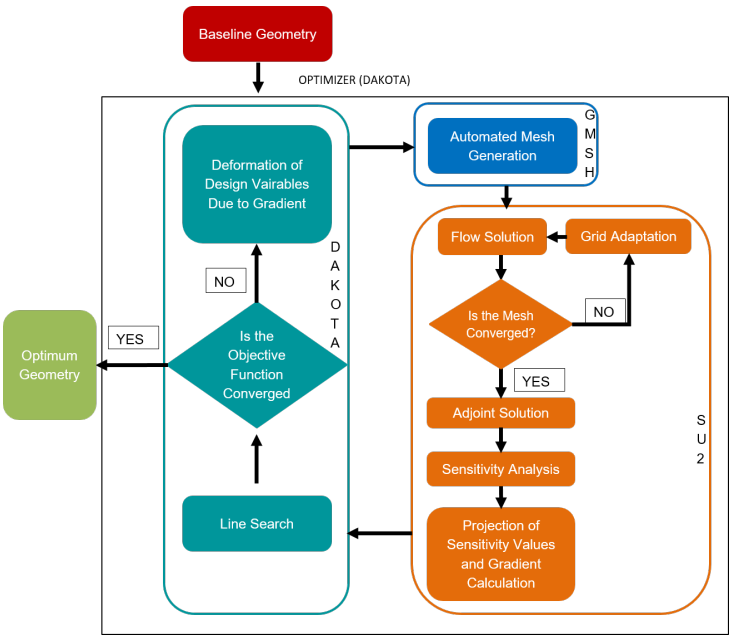

Figure 1: Optimization Framework

Optimization process is conducted by open source DAKOTA software[Adams , 2020]. A simulator script defined in DAKOTA calls mesh generation, flow solver, adjoint solver and dot product module respectively. The optimization framework is explained respectively as follows:

- Optimization process is run under DAKOTA
- Geometry is pre-defined in GMSH as a script
- GMSH creates grids at each design step.
- `SU2_CFD` performs Euler solution of flow field
- `SU2_CFD_AD` performs adjoint solution and calculates sensitivities with respect to objective function, which is C_L/C_D
- `SU2_DOT_AD` calculates gradients by performing dot product operation between sensitivities and design variables.
- DAKOTA software run optimizer with the gradient information obtained from SU^2

RESULTS AND DISCUSSION

This study is based on experiment conducted by Bergmann et al. [Bergmann, 1991]. The model dimensions are taken exactly the same with the experiment (Figure 2). Flow field is computed at $M = 0.117$ and $Re = 1.4 \cdot 10^6$ at $\alpha = 20^\circ$ by assuming as an inviscid problem. First, a mesh convergence study conducted by grid adaptation technique, then a gradient-based optimization process is employed in the study. Baseline geometry has a co-planar canard-wing layout. CL/CD is defined as the objective function and translation of canard x and z axes are assigned as design variables of the problem. Considering the canard-wing configuration, it is seen that application of the canard positively affects the pitch up moment. Therefore the optimization problem is constrained by moment coefficient, as well as the geometric boundaries.

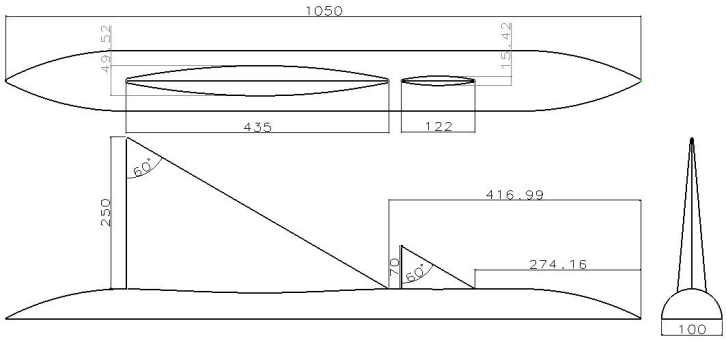

Figure 2: Delta Canard-Wing Configuration

Assessment of Solution Adaptive Grid Refinement

The capabilities of solution-based adaptive grid refinement method was discussed before by the authors, [Yutuk , 2021], for a viscous flow over the same geometry and it was concluded that this method results an efficient and accurate final mesh. Therefore, the same solution adaptive grid refinement method which based on density gradient is also employed in inviscid flow case.

Adaptation Step	Number of Tet Cells(mil)
Baseline Grid	2.399
Adaptation 1	2.638
Adaptation 2	3.024
Adaptation 3	3.553

Table 1: Cell numbers in adaptation steps

Grid adaptation is applied in three levels, each of them creating 10% new elements of the current element size. Grid adaptation is applied in three levels, each of them creating 10% new elements of the current element size. Table 1 shows the total number of cells after each adaptation level.

As seen in Figure 3, mesh refinement process especaially concentrated on vortex regions, where is actually needed to be resolved by fine cells. Then, the effect of refinement process and mesh convergence is assessed in Figure 4, by pressure coefficient distribution plots at different chordwise wing sections. Assessment of Cp plots shows that at the last two refinement level converged mesh is reached. Therefore, two level adaptation is applied in the study.

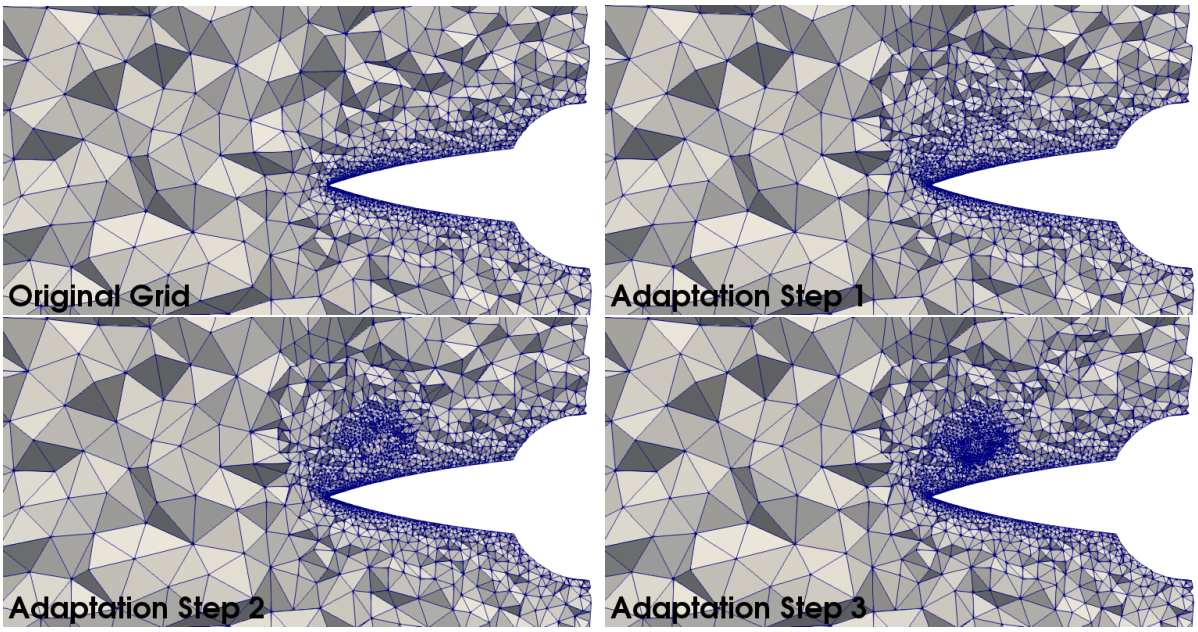

Figure 3: Grid Refinement at Each Adaptation Level

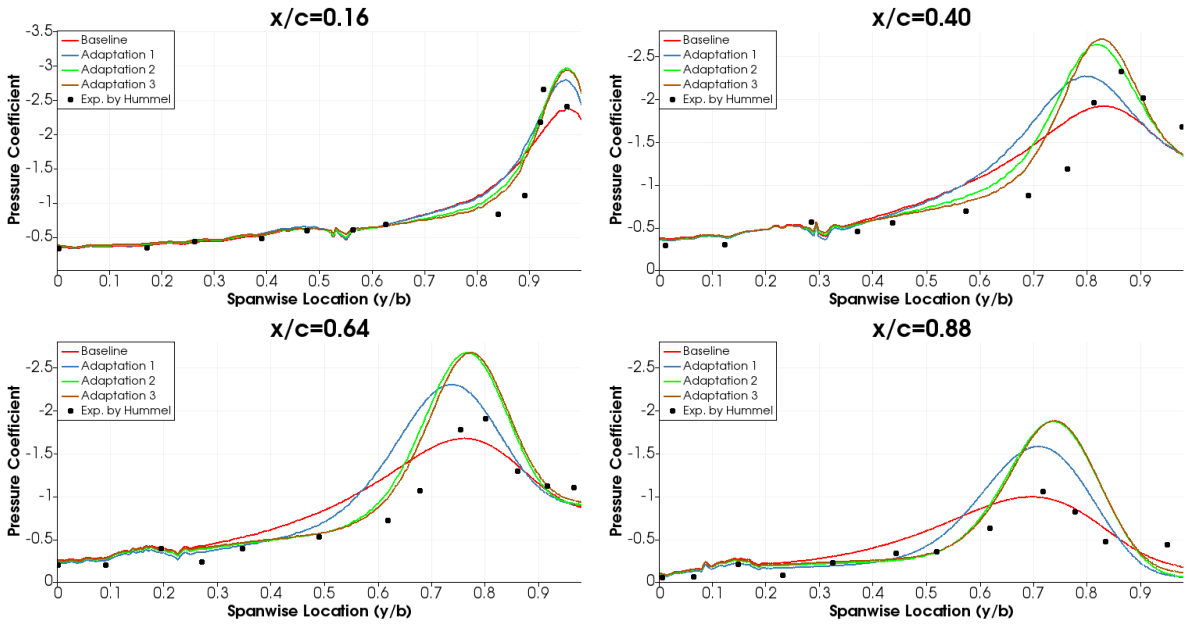

Figure 4: Cp Distribution at Different Wing Sections due to Adaptation Step

Optimization Results

Previous numerical computations showed that moving the canard may result a significant increase in pitch-up moment. Therefore, defining a moment constraint emerged as a requirement in the optimization process. As the result, the optimization problem is solved for objective function, CL/CD, employing two geometric and one nonlinear inequality constraints, which are geometric boundaries in x and z directions and moment coefficient, respectively.

Below, figures 5 and 6 show the objective function convergence history and changes in design variables and moment coefficient through the design steps. The final design provides approximately 3% improvement in objective function, while Cm is kept almost constant. Numerical solution suggests the optimum canard location by translating it approximately 0.025 m along the +z direction, and translated 0.01 m along the -x axis, as shown in red color in figure 6.

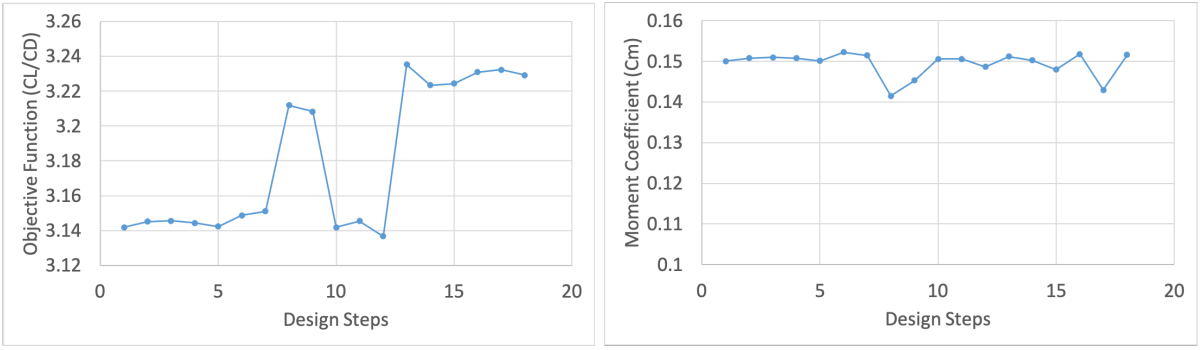

Figure 5: Delta Canard-Wing Configuration

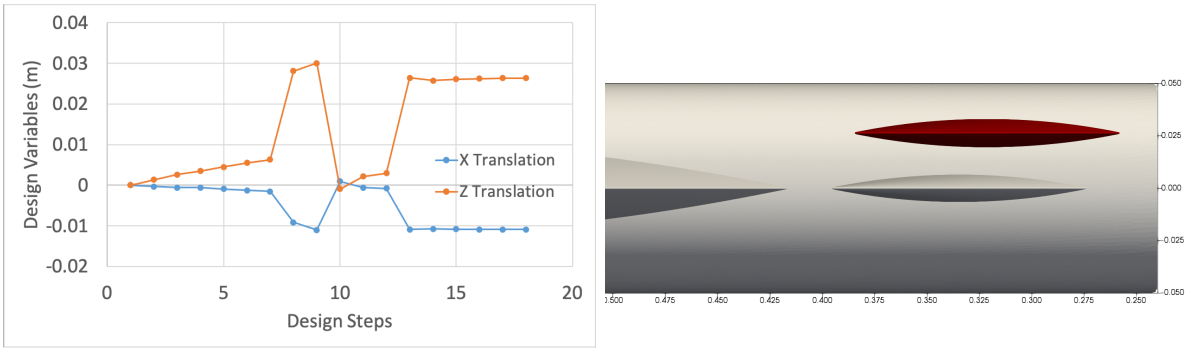

Figure 6: Delta Canard-Wing Configuration

Figure 7 shows the span-wise cp distributions on certian chord-wise sections and streamlines passing through the wing vortex core. Moving the canard upward, along +z direction, results a stronger wing vortex in inviscid simulation. There is no vortex breakdown in both cases and therefore streamlines follow a straight path. From the wing apex to wing trailing edge, each Cp distribution line reveals higher negative Cp peaks which results stronger suction over the upper surface and therefore lift increase. It also observed that, canard movement results in moving the wing vortex closer to the wing leading edge.

Below, in Figure 8, Cp distributions are plotted in the same figure. It is clearly seen that optimization process provides stronger wing vortex at each section through the wing. As stated above, as the result, C_L is increased by final design.

In below table, one can find the changes of design variables and aerodynamic coefficients. Comparing baseline and final designs reveal that optimization process kept drag and moment coefficients almost constant. On the other hand, lift coefficient is increased by approximately 2.8%. Hence, lift-to-drag ratio is also increased by approximately 2.8%

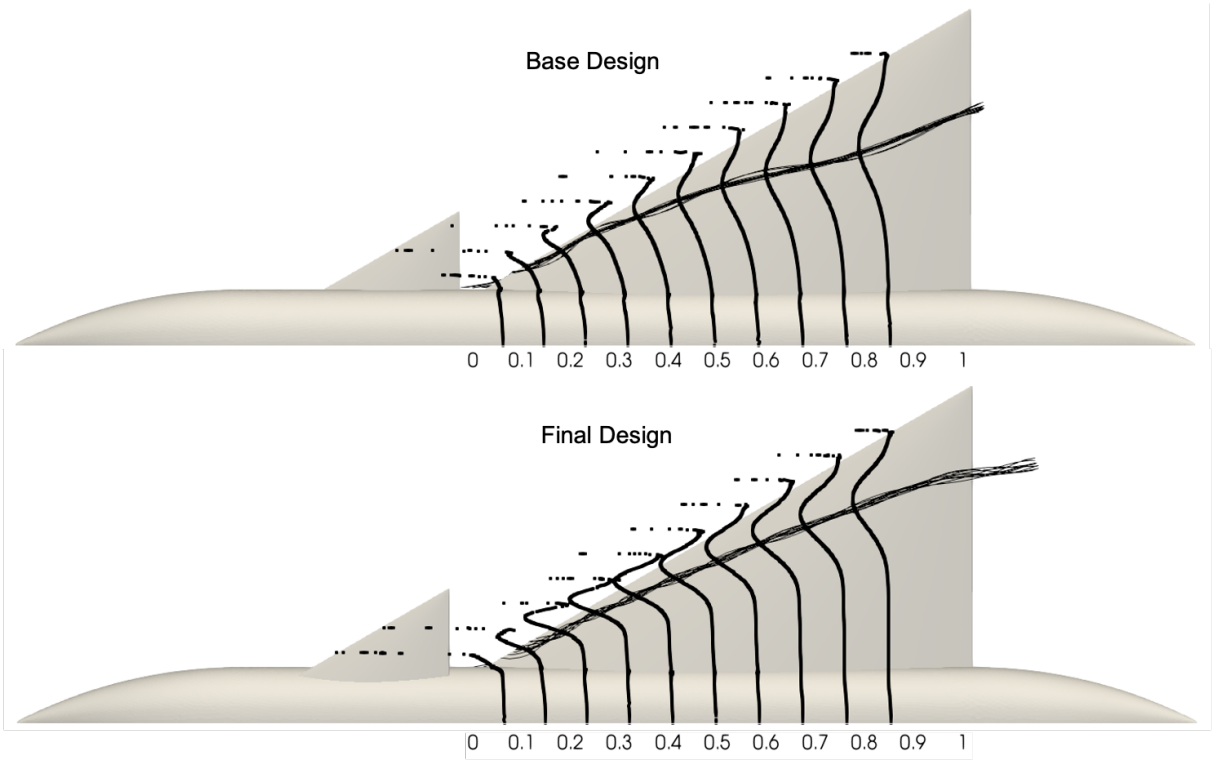

Figure 7: Cp Distributions over the Wing

Table 2: Changes in Design Variables and Aerodynamic Coefficients

	Relative X (% canard)	Relative Z (% canard)	C_L/C_D	C_L	C_D	C_{M_y}
Baseline	0.0	0.0	3.142	0.971	0.309	-0.150
Optimum	-5.12	12.67	3.229	0.999	0.310	-0.151

CONCLUSIONS

The results show that the suggesting optimization framework gives promising results for inviscid case It improves C_L about 2.8% while C_D is kept constant, thereforeC_L/C_D ratio is also improved by 2.8% at $\alpha = 20°$. C_{M_y} is defined as a constraint so that optimization process cannot provide an undesired pitch up moment at given conditions. Therefore, constraint keeps the moment coefficient almost constant through the design steps.

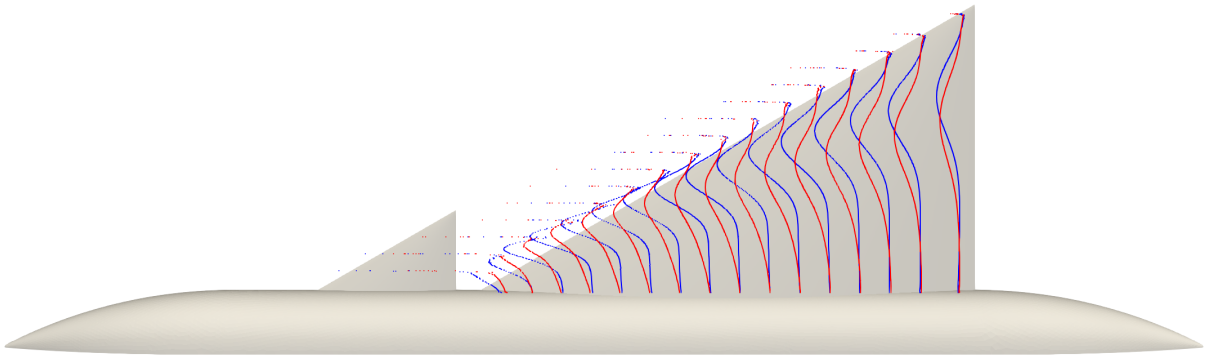

Figure 8: Cp Distributions over the Wing

References

Adams, B.M., Bohnhoff, W.J., Dalbey, K.R., Ebeida, M.S., Eddy, J.P., Eldred, M.S., Hooper, R.W., Hough, P.D., Hu, K.T., Jakeman, J.D., Khalil, M., Maupin, K.A., Monschke, J.A., Ridgway, E.M., Rushdi, A.A., Seidl, D.T., Stephens, J.A., Swiler, L.P., and Winokur, J.G., *Dakota, A Multilevel Parallel Object-Oriented Framework for Design Optimization, Parameter Estimation, Uncertainty Quantification, and Sensitivity Analysis: Version 6.12 User's Manual*, Sandia Technical Report SAND2020-12495, November 2020.

Behrbohm, H *Basic low speed aerodynamics of the short coupled canard configuration of small aspect ratio*, Svenska Aeroplan Aktiebolaget, 1965

Bergmann, A and Hummel, D and Oelker, H-Chr *Vortex formation over a close-coupled canard-wing-body configuration in unsymmetrical flow* AGARD Conference Proceedings 494, Vortex Flow Aerodynamics 14-1 - 14-14, 1991

Earnshaw, PB and Lawford, JA *Low-speed wind-tunnel experiments on a series of sharp-edged delta wings*, 1964

Gloss, B. B. *The effect of canard leading edge sweep and dihedral angle on the longitudinal and lateral aerodynamic characteristic of a close-coupled canard-wing configuration.* NASA, 1974

Gloss, B. B. *Effect of wing planform and canard location and geometry on the longitudinal aerodynamic characteristics of a close-coupled canard wing model at subsonic speeds.* NASA, 1975

Gursul, I and Yang, H *Vortex breakdown over a pitching delta wing.* Journal of fluids and structures, Elsevier, Vol 9, p:571-582, 1995

Lee, Mario and Ho, Chih-Min *Vortex dynamics of delta wings.* Frontiers in Experimental Fluid Mechanics, Springer, p:365-427, 1989

Oelker, H-Chr and Hummel, D *Investigations on the vorticity sheets of a close-coupled delta-canard configuration. Journal of aircraft.* Journal of aircraft, Vol 26, p:657-666, 1989

Palacios, Francisco & Economon, Thomas & Aranake, A.C. & Copeland, S.R. & Lonkar, Amrita & Lukaczyk, T.W. & Manosalvas-Kjono, David & Naik, Kedar & Padron, S & Tracey, Brendan & Variyar, Anil & Alonso, Juan. (2014). *Stanford University Unstructured (SU2): Open-source analysis and design technology for turbulent flows.*. 52nd Aerospace Sciences Meeting. American Institute of Aeronautics and Astronautics.

Tu, E. L. *Navier-stokes simulation of a close-coupled canard-wing-body configuration.* Journal of aircraft, Vol 29(5), p:830-838.

Tu, E. L. *Effect of canard deflection on close-coupled canard-wing-body aerodynamics.* Journal of aircraft, Vol 31(1), p:138-145.

Tu, E. L. *Numerical study of steady and unsteady Canard-Wing-Body Aerodynamics.* NASA Ames Research Center

Yutuk, K., Tikenogullari, A., and Tuncer, I. H. *Numerical investigation of vortical flows over a close-coupled delta canard-wing configuration.* Computers and Fluids, Vol 216(7) p:104822.

Biswas, R. and Strawn, R. C. *Tetrahedral and hexahedral mesh adaptation for CFD problems* Applied Numerical Mathematics Vol 26(1-2), pp:135-151

Biswas, R. and Strawn, R. C. *A new procedure for dynamic adaption of three-dimensional unstructured grids* Applied Numerical Mathematics Vol 13(6), pp:437-452